

Experimental and Computational Investigations to Explore Diverse Interactions of Vitamin C and Vitamin B Molecules Prevailing in Aqueous Mixtures of a Nerve Stimulating Drug Molecule at Different Temperatures

Paramita Karmakar¹, Biplab Rajbanshi¹, Mantu Dey¹, Ankita Shome¹, Ajit Tudu¹, Archita Paul¹, Shreya Chakraborty¹, Doli Roy¹, Priyanka Roy¹, Deepak Ekka², Mahendra Nath Roy^{1*}

¹Department of Chemistry, University of North Bengal, Darjeeling, West Bengal, India, ²Department of Chemistry, Coochbehar Panchanan Barma University, Coochbehar, West Bengal, India

ABSTRACT

In this paper, volumetric and viscometric analyses of ascorbic acid and thiamine hydrochloride in caffeine (C) aqueous solution at different mass fractions over the temperature range (298.15K–318.15K) and at 1 atm pressure have been implemented. All analyses have been interpreted in terms of solute-solute, solvent-solvent, and solute-solvent interactions of the considered system. The parameters such as apparent molar volume (ϕ_v) and limiting apparent molar volume (ϕ_v^0), have been estimated from the density data. Falkenhagen A-co-efficients and Viscosity B-co-efficients have been predicted from viscosity by implementing the Jones–Dole equation. The Hepler's constant and R_M have been evaluated. Density functional theory calculation predicts the mode of binding which correlates with the practical observations. By the help of physicochemical and computational techniques, we found that vitamins behave as structure breakers in C solution.

Key words: Apparent molar volume, DFT study, Limiting molar apparent volume, Thiamine hydrochloride, Viscosity B-co-efficients.

1. INTRODUCTION

The important nutrients of food are carbohydrates, fats, proteins, vitamins, and minerals. To increase growth and development along with carrying out the normal functions of cells and organs, our health requires relevant vitamins from food. Generally, vitamins support mental health, and immunity and also act as aides to avert some chronic diseases. The reason for diseases such as night blindness, scurvy, pellagra, beriberi, and rickets from ancient times is vitamin deficiencies. The biological as well as chemical activity along with the solvent in which they will dissolve, classify the vitamins into water-soluble and water-insoluble vitamins [1].

An important water-soluble vitamin is thiamine (B1) which exists mainly in the form of thiamine pyrophosphate salt and thiamine hydrochloride (TH) salt [Figure 1a] which is used as a dietary supplement and also in the food industry as flavor enhancer, nutritional source nutritional additive as it is not synthesized within our body [1]. It is an essential composition for genetic regulatory processes and carbohydrate metabolism due to being a coenzyme [2] and is also needed for the development of nerves and the brain [3]. Improper consumption of Vitamin B1 also affects the metabolism of carbohydrates, fat, and protein, and even causes neurologic disorders and the decay of immune function [4–6].

Another water-soluble vitamin is ascorbic acid (AA) (Vitamin C) which is also able to revive the additional antioxidants generally known as Vitamin E. Vitamin C [Figure 1b] is required for the formation of collagen and the mixture of AA with Zn is also important to heal wounds. It is also significant to synthesize of various important peptide hormones and creatinine as well as increase eyesight and delay muscular degeneration [7].

Trimethyl derivative of xanthine (2,6-di-oxopurine) is known as caffeine (C) (1, 3, 7-trimethyl xanthine) [Figure 1c], the most abundant purine alkaloid [8], naturally occurring in the foods such as coffee, tea, cacao, beans, kola, and nuts [9]. It also acts as an antioxidant and stimulant drug which affects the central nervous system [10].

The most extensively consumed drug in Western society is C. The consumption of beverages containing C causes pharmacological effects in adults as well as children. More than 80% of digested C is absorbed and dispersed to all tissues and organs. C induces hypertension, arrhythmias, altered myocardial function, increased plasma catecholamine levels, plasma renin activity, serum cholesterol levels, increased the production of urine, gastric acid secretion, and changed mood and sleep patterns.

In our present work, we have predicted the different volumetric, acoustic, and viscometric parameters of TH and AA in aqueous C ternary systems of 0.001, 0.003, and 0.005 Mol Kg⁻¹ at different solute compositions and a wide temperature range. Thus, these parameters will be very supportive to understand the mechanism of action in the system. The physicochemical and computational techniques provide

*Corresponding author:

Mahendra Nath Roy,

E-mail: mahendraroy2002@yahoo.co.in

ISSN NO: 2320-0898 (p); 2320-0928 (e)

DOI: 10.22607/IJACS.2024.1201002

Received: 10th November 2023;

Revised: 29th December 2023;

Accepted: 10th January 2024.



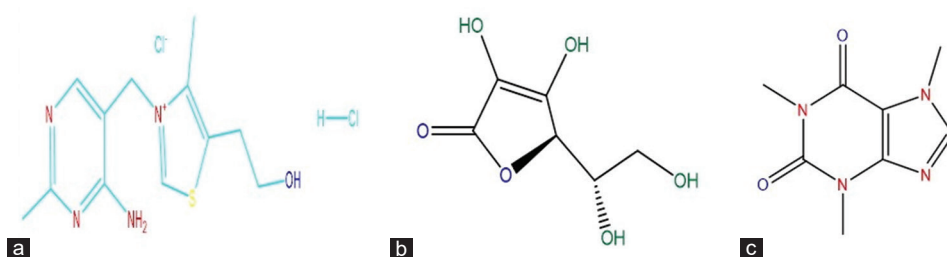


Figure 1: Chemical structure of (a) TH-HCl, (b) AA, and (c) Caffeine.

an interesting interaction phenomenon between the vitamins and aqueous stimulating drug solution to understand the effect of a drug on the vitamins.

2. EXPERIMENTAL SECTION

2.1. Materials

The studied vitamins and co-solute C were purchased from Sigma-Aldrich, Germany. The mass purity of the salts was ≥ 0.99 . The chemicals have been kept in a P_2O_5 desiccator for more than 48 h before use to reduce evaporation and contamination. The details of the used chemicals for this work are mentioned in Table 1.

2.2. Apparatus and Experimental Procedure

The required amount of weighed materials was transferred to a volumetric flask to prepare all the experimental solutions by filling with the solvents up to the mark. The evaluated uncertainty in molality of the prepared solutions is $\pm 0.0001 \text{ mol kg}^{-1}$. By the proper dilution method, the different solution sets with various concentrations were prepared for the mother solution. Mettler Toledo AG-285 with uncertainty $\pm 0.0003 \text{ g}$ was used to weigh the quantity of samples to prepare the mother solutions. The densities of the solution sets (ρ) were dignified by a vibrating-u-tube Anton Paar digital density meter (DMA 4500M) by a precision of $0.00005 \text{ g.cm}^{-3}$ maintained at $\pm 0.01\text{K}$ which was calibrated by passing dry air followed by triply distilled water. Brookfield DV-III Ultra Programmable Rheometer with spindle size 42, fitted to a Brookfield digital bath TC-500 with an accuracy of $\pm 1\%$, was utilized to estimate the viscosities of the various solution sets. The device was calibrated against the standard viscosity of the supplied samples along with it, water as well as aqueous CaCl_2 solutions. The viscosities were obtained with the help of that instrument which converts the RPM and torque into viscosities by the equation mentioned,

$$\eta = \left(\frac{100}{RPM} \right) \times T K \times torque \times SMC \quad (1)$$

The speed, spindle multiplier torque constant, and viscometer torque constant are represented by RPM, SMC (0.327), and TK (0.09373), respectively.

The refractive indices of the experimental solutions were measured with the help of a Mettler Toledo digital Refractometer with the uncertainty of ± 0.0002 units having a light with $\lambda = 589.3 \text{ nm}$. The device was calibrated twice with double distilled water and after each few measurements, it was checked. Digital METTLER TOLEDO conductivity cum pH meter with a cell constant of approximately $0.1 \pm 0.001 \text{ cm}^{-1}$ of accuracy $\pm 0.01\%$ was used to predict the conductivity of the prepared solutions. Freshly prepared 0.01 M aqueous KCl solution was used to measure the cell constant was measured. It was maintained within the range of $0.09\text{--}1.00 \text{ cm}^{-1}$ throughout the experiment at 298.15K . The temperature was maintained during the

Table 1: Chemicals name with their CAS no, mass purity, sources, and solubility.

Chemical name	CAS No	Mass purity	Sources	Solubility
Caffeine	58-08-2	$\geq 99\%$	Sigma-Aldrich	Water (Slightly hot)
Ascorbic Acid	50-81-7	$\geq 99\%$	Sigma-Aldrich	Water
Thiamine Hydrochloride	67-03-8	$\geq 99\%$	Sigma-Aldrich	Water

experiment. All the conductance data were reported with an accuracy of $\pm 0.3\%$.

2.3. Computational Details

All the density functional theory (DFT) calculations were conducted using the Gaussian 16 program [11]. Geometry optimizations of the TH, AA, C, and the composites of the binary system (TH-C and AA-C) were carried out at B3LYP/6-31++G(d,p) level of theory. To corroborate the geometries of the ground state and constitute the global minima on the potential energy surfaces vibration frequency analysis was executed at the same level. To detain the type of interactions occurring inside the systems, the composites molecular electrostatic potential (MEP) maps were generated at the same level of theory. Finally, energies of binding or adsorption (ΔE_{ads}) for all components were estimated by the following formula:

$$\Delta E_{ads}(\text{TH-C}) = E_{\text{TH-C}} - E_{\text{TH}} - E_{\text{C}}$$

$$\Delta E_{ads}(\text{AA-C}) = E_{\text{AA-C}} - E_{\text{AA}} - E_{\text{C}}$$

Here, $E_{\text{TH-C}}$ and $E_{\text{AA-C}}$ are the total energy of the geometry-optimized composites whereas E_{TH} , E_{AA} , and E_{C} are the optimized energy for free states accordingly.

3. RESULTS AND DISCUSSION

3.1. Density and Volumetric Measurement

The facts concerning the interaction of Vitamin C in solutions where water was used as a solvent have been attained from the apparent molar volume (ϕ_v), limiting apparent molar volume (ϕ_v^0), and experimental slope (S_v^*). Since the solute species migrated inside the solvent habitat are governing all these mentioned parameters which shield all the information belong to the structural penalties of interactions between solute and solvent [12]. The solute-solvent interaction with the co-solvent implies the apparent molar volume. Densities of the mentioned vitamins in C-water solution system with various mass fractions were measured at temperature series, $288.15\text{--}318.15(\phi_v)$, having different concentrations, were predicted using the following equation [13-17] with the help of density (ρ) data [Tables S1 and S2],

$$\phi_v = \frac{M}{\rho} - \frac{1000(\rho - \rho_0)}{m\rho\rho_0} \quad (2)$$

where, M , m , ρ , and ρ_0 denote their usual meaning [18]. Using the following relation [18], the molality of all the systems (m) has been calculated from the density (ρ) data and molar (c) concentration. The positive values as well as higher magnitudes of ϕ_v suggest that there are strong interactions among the solute and the solvent molecules. There is a descending nature of ϕ_v values with the increase in the concentration of the vitamins [Figures S1 and S2]. Using the least squares fitting of linear plots of (ϕ_v) against the square root of molar concentrations (\sqrt{m}) is utilized to measure the limiting molar apparent volume (ϕ_v^0), means, apparent molar volume at infinite dilution and experimental slopes (S_v^*) with the help of Masson equation [19,20].

Table 2: Apparent molar volume (ϕ_v^0), S_v^* , molar refraction (R_M^0), and viscosity- A and viscosity- B co-efficient of (TH+H₂O+CAFFEINE), and (AA+H₂O+CAFFEINE) systems in solution of C of mass fractions $w_1=0.001$, $w_2=0.003$, $w_3=0.005$, at 288.15K, 298.15K, 308.15K, and 318.15 K.

T (K ^b)	$\phi_v^0 \times 10^6 / \text{m}^3 \text{mol}^{-1}$	$S_v^* \times 10^6 / \text{m}^3 \text{mol}^{-3/2} \text{kg}^{1/2}$	$R_M^0 / \text{m}^3 \text{mol}^{-1}$	A	B
TH+H₂O+CAFFEINE					
$w_1=0.001$					
288.15	154.18	-44.921	39.72	0.2663	0.471
298.15	158.39	-47.202	39.80	0.0120	0.711
308.15	164.62	-54.916	39.95	0.0685	0.7201
318.15	171.04	-107.21	40.05	0.8148	0.9166
$w_2=0.003$					
288.15	155.09	-49.219	39.75	0.2301	0.6254
298.15	159.73	-56.976	39.80	0.0321	0.7697
308.15	165.18	-59.063	39.95	0.0496	0.9063
318.15	172.1	-110.3	40.08	0.8806	1.1200
$w_3=0.005$					
288.15	156.31	-67.408	39.83	0.2272	0.7866
298.15	161.13	-68.927	39.92	0.0166	0.9378
308.15	166.35	-69.498	40.05	0.0438	1.0111
318.15	173.4	-125.57	40.18	0.8605	1.2088
AA+H₂O+CAFFEINE					
$w_1=0.001$					
288.15	166.84	-33.483	35.81	0.2677	0.3747
298.15	168.49	-17.164	35.84	0.0895	0.4539
308.15	171.62	-36.969	35.93	0.3266	0.6101
318.15	176.28	-25.733	36.00	0.9355	0.9591
$w_2=0.003$					
288.15	167.85	-38.587	36.11	0.4470	0.4907
298.15	171.05	-39.105	36.14	0.0402	0.7593
308.15	175.84	-70.654	36.23	0.2972	0.8843
318.15	182.76	-49.212	36.31	0.8982	0.9912
$w_3=0.005$					
288.15	169.48	-42.24	36.13	0.4618	0.5619
298.15	173.15	-56.815	36.16	0.0292	0.8435
308.15	176.18	-80.434	36.25	0.2798	0.9619
318.15	183.74	-59.38	36.33	0.9512	1.017

^aStandard uncertainties in mass fraction u (w) = ±0.0001 mol kg⁻¹

$$\phi_{ii} = \phi^0 + S^* \cdot \sqrt{m} \quad (3)$$

The values of (ϕ_v^0) and (S_v^*) of each and every vitamin are shown in Table 2. [Figures S1 and S2] have contained all the values of (ϕ_v^0) and (S_v^*) of each and every vitamins which came from the experimental plot, determined from the Masson equation. All positive values of (ϕ_v^0) are positive for all ternary systems supporting the solute-solvent interaction.

The dipole-dipole interaction inside the solution systems, explains the difference of solute-solvent interactions, and the larger the dipole-dipole interaction smaller will be the ϕ_v as well as ϕ_v^0 -values [21].

In addition, the ascending order of the values of ϕ_v^0 with the increase in temperature along with mass fraction of C prefers the increasing shift

of solute-cosolute interaction. During the occurrence of interactions, there is some space inside the solvent particles occupied by the solute particles by the loose solvation layer which properly explains this trend. The possibility of ion-ion interaction inside the solution system is assigned with the experimental slope values and the negative S_v^* values indicate the lesser interaction in that solvent media. The dominating factor is ϕ_v^0 which explains the solute-solvent interaction and the greater magnitude of ϕ_v^0 than S_v^* considers the dipole-solvent interaction and violets the dipole-dipole interaction [22]. Hence, it might be said that the solute-solute interaction is predominated by the solute-solvent interaction.

3.1.1 The temperature effect on ϕ_v^0

ϕ_v^0 , the individual apparent molar volume at infinite dilution was studied at different temperature ranges at the interval of 10K, and all results were obtained with the help of the following polynomial equations [23],

$$\phi_v^0 = a_0 + a_1 T + a_2 T^2 \quad (4)$$

$$\phi_E^0 = (\delta\phi_v^0/\delta T)_P = a_1 + 2a_2 T \quad (5)$$

$$(\delta\phi_E^0/\delta T)_P = (\delta^2\phi_v^0/\delta T^2)_P = 2a_2 \quad (6)$$

Here, a_0 , a_1 , and a_2 signify the empirical co-efficients which mainly depend on the solute's nature and Table 3 covers all the values of the co-efficient [Figure 2]. Equation (6) predicts the values of limiting

Table 3: Values of empirical co-efficients

(a_0 , a_1 , and a_2) of Eq. 5 for aqueous (TH+H₂O+CAFFEINE) and (AA+H₂O+CAFFEINE) systems solution of caffeine of different mass fraction $w_1=0.001$, $w_2=0.003$, and $w_3=0.005$ at 288.15K, 298.15K, 308.15K, and 318.15 K.

Mass fraction	$a_0 \times 10^6 / \text{m}^3 \text{ mol}^{-1}$	$a^1 \times 10^6 / \text{m}^3 \text{ mol}^{-1} \text{ K}^{-1}$	$a^2 \times 10^6 / \text{m}^3 \text{ mol}^{-1} \text{ K}^{-2}$
TH+H₂O+CAFFEINE			
0.001	496.89	-2.7817	0.0055
0.003	514.92	-2.8911	0.0057
0.005	504.69	-2.8152	0.0056
AA+H₂O+CAFFEINE			
0.001	766.37	-4.2479	0.0075
0.003	877.76	-5.1434	0.0093
0.005	929.28	-5.4382	0.0097

Table 4: Values of limiting apparent molar expansibilities (ϕ_E^0) of (TH+H₂O+CAFFEINE) and (AA+H₂O+CAFFEINE) systems in a solution of caffeine of different mass fraction $w^1=0.001$, $w^2=0.003$, and $w^3=0.005$ at 288.15K, 298.15K, 308.15K, and 318.15 K.

Mass fraction (w)	$\phi_E^0 \times 10^6 / \text{m}^3 \text{ mol}^{-1} \text{ K}^{-1}$			$(\delta\phi_E^0/T)_P \times 10^6 / \text{m}^3 \text{ mol}^{-1} \text{ K}^{-2}$	
TH+H ₂ O+CAFFEINE	288.15K	298.15K	308.15K	318.15K	
0.001	0.38795	0.49795	0.60795	0.71795	0.011
0.003	0.39381	0.50781	0.62181	0.73581	0.0114
0.005	0.41208	0.52408	0.63608	0.74808	0.0112
AA+H₂O+CAFFEINE					
0.001	0.07435	0.22435	0.37435	0.52435	0.0150
0.003	0.21619	0.40219	0.58819	0.77419	0.0186
0.005	0.15191	0.34591	0.53991	0.73391	0.00194

apparent molar expansibilities (ϕ_E^0) at different temperatures which are also listed in Table 4.

The positive value of all the limiting apparent molar expansibilities (ϕ_E^0) indicates the absence of a caging effect among molecules for all the solution systems.

Hepler had developed a way to predict the solute-solvent interaction, to indicate the structure breaker or structure maker interaction which actually occurs in the solution phase [24]. $(\delta\phi_E^0/\delta T)_P$ value mainly determines whether the system is structure destructor or structure maker interaction [25], according to Hepler. Usually, the interaction inside the system will be structure-making if $(\delta\phi_E^0/\delta T)_P$ value is negative or very small, and on the other hand, structure breaking if the value is positive or large. All positive and small values of $(\delta\phi_E^0/\delta T)_P$ are listed in Table 4 distinctly stipulating the way of interaction is nothing but structure making.

3.2. Viscosity and the Co-efficients of Viscosity

The investigation of the co-efficient of viscosity at different temperatures along with the different concentrations of the aqueous solution of vitamins describes easily the region of both the constitutional interaction [26-28] as well as the solvation [29] within the co-spheres [30] inside the solution.

The values of viscosities of the solution systems for several concentrations and temperatures are obtained experimentally [Table S3]. Using the following Jones-Dole equation [31] with the help of these viscosities data, viscosity co-efficients are obtained.

$$\eta_r = \frac{\eta}{\eta_0} = 1 + A\sqrt{c} + Bc \quad (7)$$

$$\frac{\eta_r - 1}{\sqrt{c}} = A + B\sqrt{c} \quad (8)$$

Here, “c” is the molality (concentration) η and η_r are signifying their usual meaning [32]. We get equation (9) by rearranging equation (8), where A co-efficients represents the long-range coulombic forces, well known as Falken-Hagen co-efficient [33] stands for solute-solute interaction in solution. Oppositely, the degree of the effective hydrodynamic volume is designated by B -co-efficient generally represents the solute-solvent interaction and the magnitude of the B-co-efficient depends on the shape, size, and partial molar entropies of the solutes.

The values of A and B co-efficients are got from the different plots of $(\eta_r - 1)/\sqrt{c}$ vs. \sqrt{c} [Table S5, Figures S3, and S4] with the help of linear

square analysis which is given in Table 2. Actually, the value of the intercept and experimental slope of plots are the viscosity A and B co-efficient, respectively.

From the values of viscosity B co-efficient at different temperatures and different mass fractions, it is able to us to determine the order of solute-solvent interaction as concluded above [Figure 3] [27,34,35].

3.2.1. The effect of temperature on viscosity co-efficient B

To explain the nature of solute-solvent interaction as synergistic structure breaker or structure maker, the immeasurable study of viscosity B co-efficient is reformed which is mainly the first order derivative of B co-efficient over the temperature range. (dB/dT) describes the activation energy which is required for the viscous flowing in the solution, mainly the quantity of chaotropic. (dB/dT) authentically signifies the structure-making or breaking phenomena [36-39].

The small positive and negative value of the derivative part suggests the structure maker whereas structure maker is indicated by the large positive value. All values of (dB/dT) with a mass fraction of co-solutes are given in the following Table 5.

3.3. Refractive Index and the Molar Refractions

The optical instruction of the refractive index of the homogeneous mixture has contributed fascinating information about the molecular

interactions, that is, the qualitative structure of solutions systems. With the help of the composition-dependent polynomial equation and from the Lorentz-Lorenz relation [40,41], R_M (molar refraction) in the systems can be predicted.

$$R_M = \frac{(n_D^2 - 1)}{(n_D^2 + 2)} \left(\frac{M}{\rho} \right) \quad (9)$$

Here, R_M , n_D , M , and ρ are bearing their usual significance. The refractive index of that system is mainly the ability to refract the light of a system and as a consequence, estimate the solid behavior of that system. The refractive indices (n_D) of all the homogeneous systems are already reported in Table 2. The molar refraction (R_M) of the considered solutions was evaluated and enlisted [Table S4] for all systems.

Table 5: Values of dB/dT for $(TH+H_2O+CAFFEINE)$ and $(AA+H_2O+CAFFEINE)$ systems in different mass ($w=0.001, 0.003, 0.005$) fractions of aqueous C solution at 288.15 to 318.15 K.

Mass fraction	0.001	0.003	0.005
$TH+H_2O+CAFFEINE$	0.0135	0.0162	0.0134
$AA+H_2O+CAFFEINE$	0.0191	0.0163	0.0148

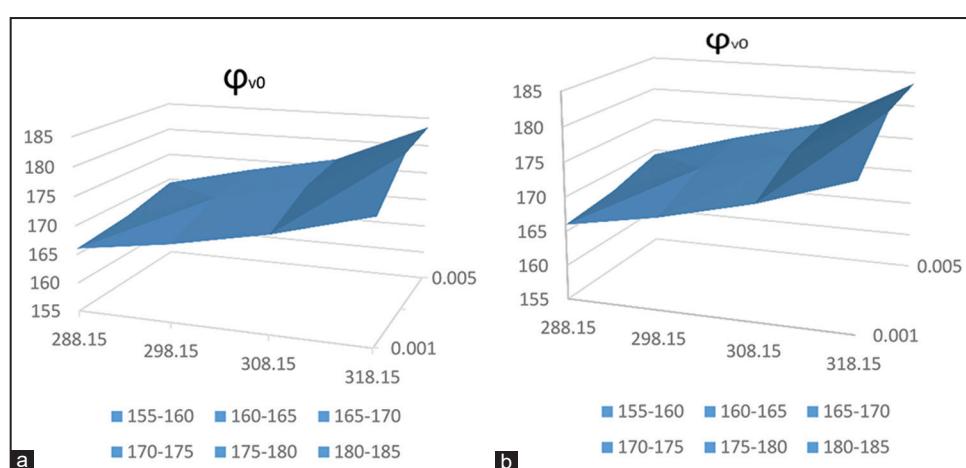


Figure 2: Plot of φ_v versus \sqrt{m} of $w=0.001, 0.003, 0.005$ for (a) $(TH+H_2O+CAFFEINE)$ (b) $(AA+H_2O+CAFFEINE)$ at 288.15K, 298.15K, 308.15K, and 318.15K.

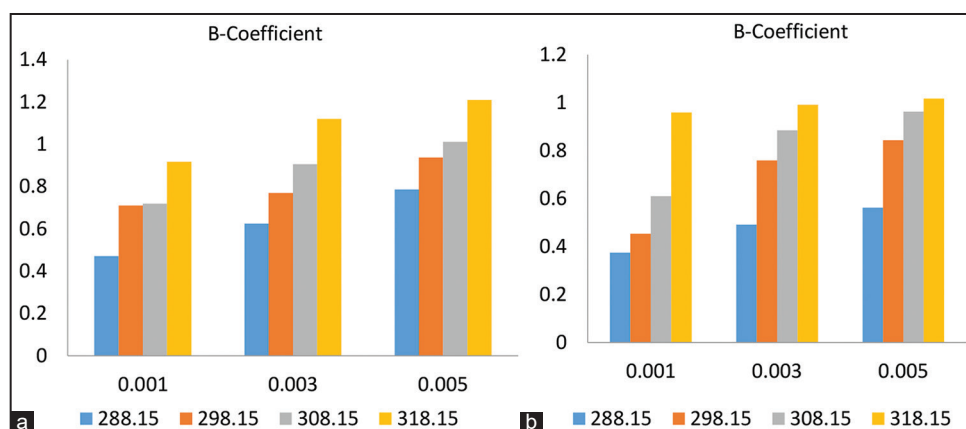


Figure 3: Plot of B -co-efficient versus \sqrt{m} of $w=0.001, 0.003, 0.005$ for (a) $(TH+H_2O+CAFFEINE)$ (b) $(AA+H_2O+CAFFEINE)$ at 288.15K, 298.15K, 308.15K and 318.15K.

The limiting molar refraction, (R_M^0) values listed in Table 1 can be estimated using the equation mentioned below,

$$R_M = R_M^0 + R_S \sqrt{m} \quad (10)$$

Where, R_M^0 implicates the solvent-solute interaction while "m" is the molality (concentration) of the solution. Hence, this measurement

is the intense implement to explain the molecular interaction in solution. The ascending order in the values of R_M [Table S4] along with R_M^0 [Table 2 and Figure 4] and [Figure S5 and S6] within a mass fraction of the co-solvent also indicates that solute-solvent interaction is predominated which is also reinforced by the viscosity as well as density analysis.

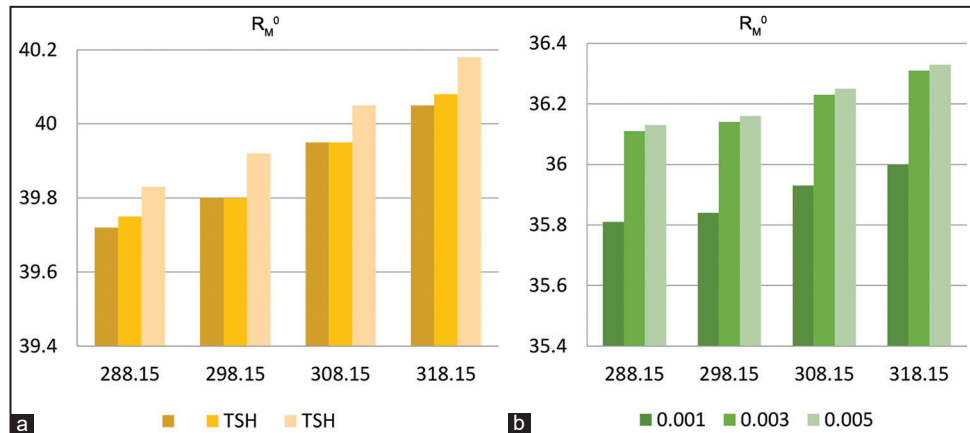


Figure 4: Plot of R_M^0 versus \sqrt{m} of $w=0.001, 0.003, 0.005$ for (a) (TH+H₂O+CAFFEINE) (b) (AA+H₂O+CAFFEINE) at 288.15K, 298.15K, 308.15K, and 318.15K.

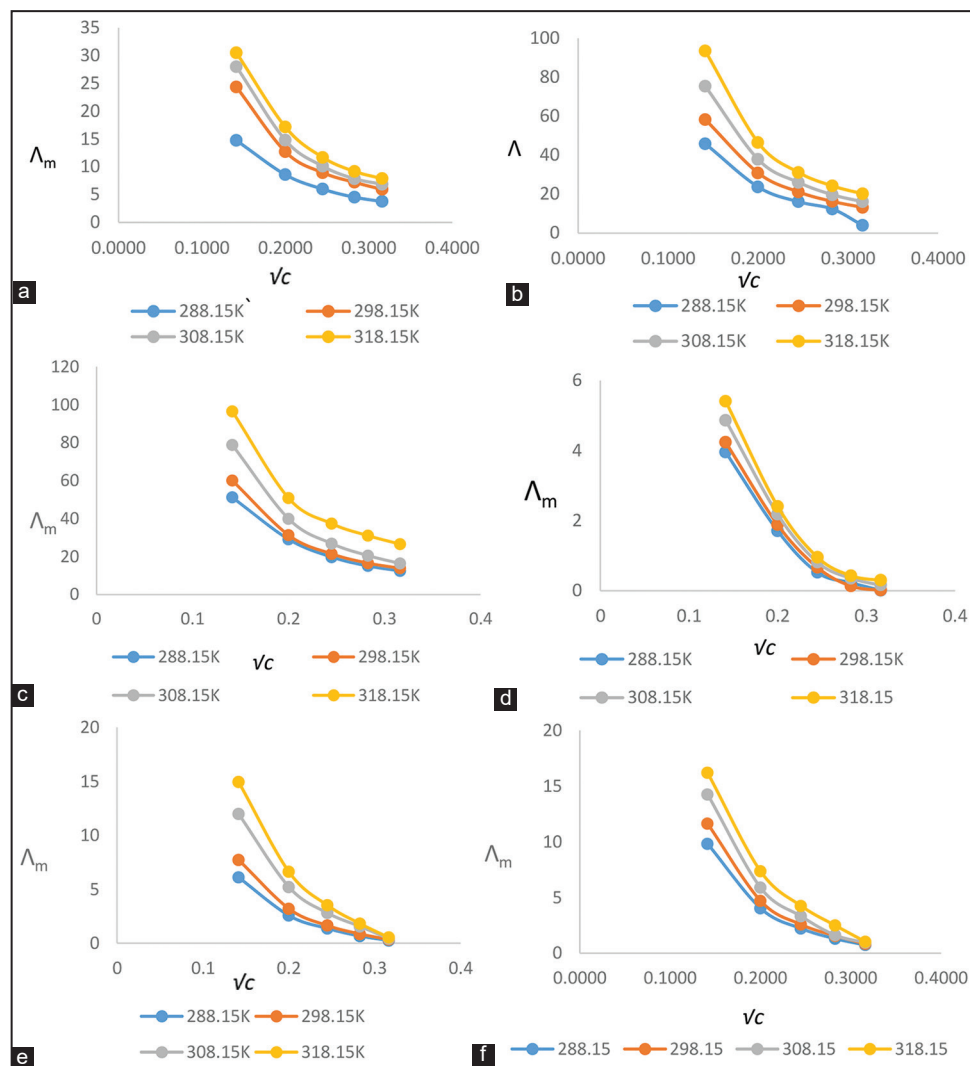


Figure 5: Plot of molar conductivity (Λ_m) versus \sqrt{c} of (a-c)(TH+H₂O+CAFFEINE) (d-f) (AA+H₂O+CAFFEINE) systems in aqueous caffeine solutions of mass fractions $w_1=0.001$ $w_2=0.003$, and $w_3=0.005$ at 288.15K, 298.15K, 308.15K, and 318.15K.

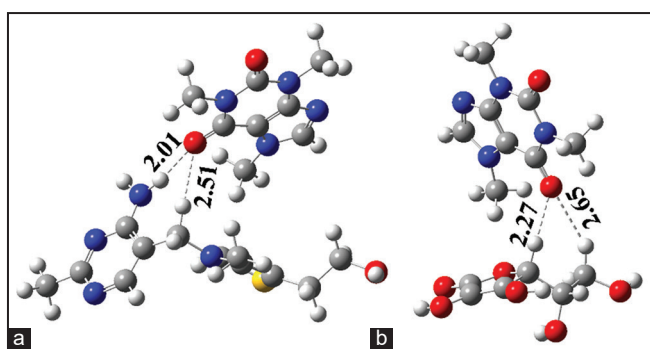


Figure 6: Optimized geometries for the (a) TH-C (b) AA-C, where red, gray, white, blue, and yellow colors represent oxygen, carbon, hydrogen, nitrogen, sulfur, and atoms, respectively.

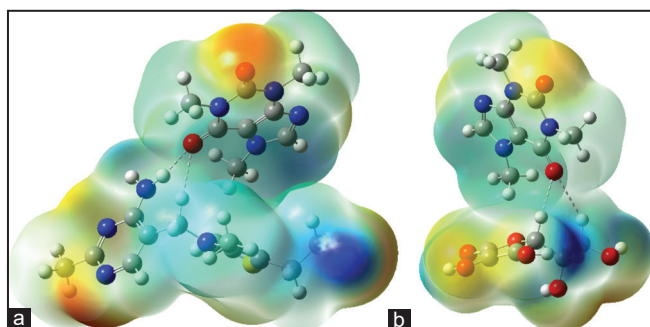
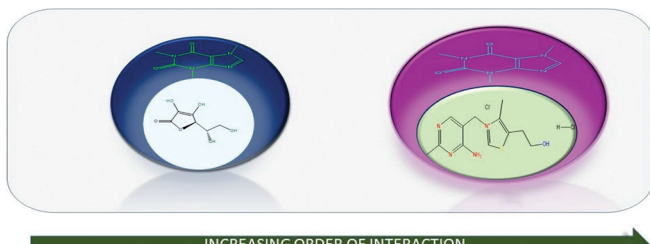


Figure 7: Electrostatic potential maps for (a) TH-C (b) AA-C.



Scheme 1: Increasing order of interaction between ascorbic acid and thiamine hydrochloride in caffeine (C) aqueous solution.

The observed results help to arrange the most probable order of the chosen systems which is represented in Scheme 1.

3.4. Conductivity Study

The interaction along with the mobility phenomena of the systems are given by the conductivity measurement [42].

The molar conductivities [43] (Λ_m) of the solutions at different mass fractions have been given [Table S6]. The following figures are showing the resulting plots of the respective systems [Figure 5]. The mobility of the corresponding species in solutions playing the leading role, Λ_m increases with the rise of mass fraction in the same system. It might be due to the larger solute-solvent interaction which is governed by the dipole-dipole interaction (H-bonding) in homogeneous mixtures among the solute and solvent molecules. The molecular assembly formation gives the driving forces to the species to lose their independent mobility to make the species less mobile to give conductivity in the solution. Thus, this study supports the refractometric, volumetric, and viscometric studies.

3.5. Theoretical Study of Solute-Solvent Interaction

We have carried out DFT calculations to predict the type of interaction between solute and solvent employed in the composite systems using the following theoretical observations. Figures 6a and b indicate the optimized ground state geometries of the TH-C and AA-C composition, respectively. Here, TH-C complex feels a stronger attraction as well as a shorter hydrogen-bond distance of 2.01, 2.51 Å along with respect to the corresponding AA-C (2.27, 2.65 Å). Consequently, C weakly interacts with AA (Eads = -21.35 kJ/mole) while the TH offering relatively higher adsorption energy (Eads = -22.68 kJ/mole).

To analyze electrostatic interactions between the composites, MEP is plotted as mentioned in Figure 7. The prominent orange region of MEP maps for TH-C and AA-C indicates the electrostatic interaction is developed in electronegative oxygen atoms while blue regions are operating in electropositive hydrogen atoms. This observation is conformable to the practical findings.

4. CONCLUSION

The density, viscosity, and refractive index have studied of the ternary solutions of TH+H₂O+CAFFEINE, AA+H₂O+CAFFEINE at 288.15K, 298.15K, 308.15K, and 318.15K in aqueous C solvent of different concentration. The study leads to the conclusion that solute-solvent interaction is predominant over the solute-solute interaction and most of the experimental parameters indicate solute-solvent interaction is higher in the case of TH+H₂O+CAFFEINE than AA+H₂O+CAFFEINE which is supported by the trend in adsorption energies of these species in C. One plausible reason for the trends of the observation is the possibility of H-bonding. This result indicates that TH and AA both can easily penetrate into the accumulated C solution. This fact is also supported by our theoretical study. These observations have immense importance to understand the vitamin-solvent interaction.

5. ACKNOWLEDGMENT

This work was supported by the University Grant Commission, New Delhi, India (No. 540/27/DRS/2007, SAP-1). Prof. M.N. Roy (FRSC LONDON) is grateful to the UGC, New Delhi, Government of India, for being awarded a 1-time grant under the Basic Scientific Research through the Grant-in-Aid no. F4-10/2010 (BSR) regarding his active service for augmenting research facilities to facilitate further research work.

6. REFERENCES

1. S. S. Dhondge, P. N. Dahasahasra, L. J. Paliwal, V. M. Tangde, D. W. Deshmukh, (2017) Volumetric and viscometric study of thiamine hydrochloride, pyridoxine hydrochloride and sodium ascorbate at T = (275.15, 277.15 and 279.15) K in dilute aqueous solutions, *The Journal of Chemical Thermodynamics*, **107**: 189-200.
2. D. Lonsdale, (2006) A review of the biochemistry, metabolism and clinical benefits of thiamin(e) and its derivatives, *Evidence-based Complementary and Alternative Medicine*, **3**: 49-59.
3. L. Bettendorff, M. Peeters, P. Wins, E. Schoffeniels, (1993) Metabolism of thiamine triphosphate in rat brain: Correlation with chloride permeability, *Journal of Neurochemistry*, **60**: 423-434.
4. H. R. Horton, L. A. Moran, R. S. Ochs, J. D. Rawn, K. G. Scrimgeour, (1996) *Principles of Biochemistry*, Hoboken: Prentice Hall.
5. J. Phoenix, P. Hopkins, C. Bartram, R. J. Beynon, R. C. Quinlivan, R. H. Edwards, (1998) Effect of vitamin B6 supplementation



- in McArdle's disease: A strategic case study, *Neuromuscular Disorders*, **8**: 210-212.
6. K. Shibata, T. Tsuji, T. Fukuwatari, (2013) Intake and urinary amounts of biotin in Japanese elementary school children, college students, and elderly persons. *Nutrition and Metabolic Insights*, **6**: 43-50.
 7. M. N. Roy, R. K. Das, A. Bhattacharjee, (2010) Apparent molar volume, viscosity B-coefficient, and adiabatic compressibility of tetrabutylammonium bromide in aqueous ascorbic acid solutions at $T = 298.15, 308.15$, and 318.15 K , *Russian Journal of Physical Chemistry A*, **84**: 2201.
 8. Merck and Co-Inc., (2001) *The Merck Index*, New Jersey: White House Station.
 9. A. Pedronel, C. Herley, O. Carlos, H. Beatriz, (2007) Insedical activity. Caffeine aqueous solutions, *Journal of Agricultural and Food Chemistry*, **55**(17): 6918-6922.
 10. C. E. Ana, I. A. V. Cecilia, M. M. Victor, M. T. O. P. V. Ana, J. B. Francisco, A. Miguel, (2009) Diffusion coefficients of the ternary system at 298.15K , *Journal of Chemical and Engineering Data*, **54**: 115-117.
 11. M. Frisch, G. Trucks, H. Schlegel, G. Scuseria, M. Robb, J. Cheeseman, G. Scalmani, V. Barone, G. Petersson, H. Nakatsuji, (2016) *Gaussian 16, Revision B.01*, Wallingford, CT: Gaussian Inc. [12a] Y. Gao, H. Liu, S. Zhang, Q. Gu, Y. Shen, Y. Ge, B. Yang B, (2018) Excimer formation and evolution of excited state properties in discrete dimeric stacking of an anthracene derivative: A computational investigation, *Physical Chemistry Chemical Physics*, **20**(17): 12129-12137. [12b] S. Grimme, (2011) Density functional theory with London dispersion corrections, *WIREs Computational Molecular Science*, **1**: 211-228.
 12. M. N. Roy, R. Chanda, R. K. Das, D. Ekka, (2011) Densities and viscosities of citric acid in aqueous cetrimonium bromide solutions with reference to the manifestation of solvation, *Journal of Chemical and Engineering Data*, **56**: 3285-3290.
 13. E. Ayrancı, (1997) Apparent molar volume and viscosity of compounds with asymmetric carbon atoms, *Journal of Chemical and Engineering Data*, **42**: 934-937.
 14. Z. Yan, J. Wang, J. Lu, (2001) Apparent molar volumes and viscosities of some α -amino acids in aqueous sodium butyrate solutions at 298.15 K , *Journal of Chemical and Engineering Data*, **46**: 217-222.
 15. Y. Li, X. Wang, Y. Wang, (2006) Comparative studies on interactions of bovine serum albumin with cationic Gemini and single-chain surfactants, *The Journal of Physical Chemistry B*, **110**: 8499-8505.
 16. M. T. Zafarani-Moattar, H. Shekaari, P. Jafari, (2019) Thermodynamic study of aqueous two-phase systems containing biocompatible cholinium aminoate ionic-liquids and polyethylene glycol dimethyl ether 250 and their performances for bovine serum albumin separation, *The Journal of Chemical Thermodynamics*, **130**: 17-32.
 17. P. Karmakar, D. Das, B. Rajbanshi, D. Roy, S. Ray, N. Ghosh, A. Roy, S. Ghosh, D. Ekka, A. Sharma, M. N. Roy, (2022) Physicochemical and computational investigations of some food chemicals prevalent in aqueous 1-butyl-1-methyl-pyrrolidinium chloride solutions with the manifestation of solvation consequences, *Journal of Molecular Liquids*, **353**: 0167-7322.
 18. S. E. Friberg, (1994) Interactions of surfactants with polymers and proteins. E. D. Goddard and K. P. Ananthapadmanabhan (Eds.), CRC Press, Boca Raton, FL, 1993, pp. 1-427, \$169.95, *Journal of Dispersion Science and Technology*, **15**: 399.
 19. V. Minkin, O. Osipov, Y. Zhdanov, (1970) *Dipole Moments in Organic Chemistry*, New York: Plenum Press.
 20. K. Kumar, S. Chauhan, (2015) Surface tension and UV-visible investigations of aggregation and adsorption behavior of NaC and NaDC in water-amino acid mixtures, *Fluid Phase Equilibria*, **394**: 165-174.
 21. G. Ravichandran, G. Lakshminarayanan, D. Ragouramane, (2013) Apparent molar volume and ultrasonic studies on some bile salts in water-aprotic solvent mixtures, *Fluid Phase Equilibria*, **356**: 256-263.
 22. D. Ekka, M. N. Roy, (2013) Molecular interactions of alpha-amino acids insight into aqueous beta-cyclodextrin systems, *Amino Acids*, **45**: 755-777.
 23. M. N. Roy, V. K. Dakua, B. Sinha, (2007) Partial molar volumes, viscosity B-coefficients, and adiabatic compressibilities of sodium molybdate in aqueous 1,3-dioxolane mixtures from 303.15 to 323.15 K , *International Journal of Thermophysics*, **28**: 1275-1284.
 24. Y. Zhang, P. S. Cremer, (2006) Interactions between macromolecules and ions: The Hofmeister series, *Current Opinion in Chemical Biology*, **10**: 658-663.
 25. A. Yasmin, S. Barman, B. K. Barman, M. N. Roy, (2018) Investigation of diverse interactions of amino acids (Asp and Glu) in aqueous Dopamine hydrochloride with the manifestation of the catecholamine molecule recognition tool in solution phase, *Journal of Molecular Liquids*, **271**: 715-729.
 26. P. K. Banipal, T. S. Banipal, J. C. Ahluwalia, B. S. Lark, (2000) Partial molar heat capacities and volumes of transfer of some saccharides from water to aqueous urea solutions at $T= 298.15\text{ K}$, *The Journal of Chemical Thermodynamics*, **32**: 1409-1432.
 27. H. D. B. Jenkins, Y. Marcus, (1995) Viscosity B-coefficients of ions in solution, *Chemical Reviews*, **95**: 2695-2724.
 28. H. T. Briscoe, W. T. Rinehart, (1942) Studies of relative viscosity of non-aqueous solutions, *The Journal of Physical Chemistry*, **46**: 387-394.
 29. H. Eisenberg, (1968) Chemical physics of ionic solutions. B. E. Conway and R. G. Barradas, Eds., Wiley, New York, 1966. 622 pp. \$25.00, *Journal of Polymer Science Part A-2: Polymer Physics*, **6**: 1943.
 30. G. W. Brady, J. T. Krause, (1957) Structure in ionic solutions. I, *The Journal of Chemical Physics*, **27**: 304-308.
 31. G. Jones, M. Dole, (1929) The viscosity of aqueous solution of strong electrolysis with special reference to barium chloride, *Journal of the American Chemical Society*, **51**: 2950-2964.
 32. B. Rajbanshi, K. Das, K. Lepcha, S. Das, D. Roy, M. Kundu, M. N. Roy, (2019) Minimization of the dosage of food preservatives mixing with ionic liquids for controlling risky effect in human body: Physicochemical, antimicrobial and computational study, *Journal of Molecular Liquids*, **282**: 415-427.
 33. A. Ali, S. Hyder, Y. Akther, (2005) Viscometric studies of a -amino acid in aqueous NaCl and MgCl_2 at 303 K , *Indian Journal of Physics*, **79**: 157-160.
 34. Y. Marcus, (1994) Viscosity B-coefficients, structural entropies and heat capacities, and the effects of ions on the structure of water, *Journal of Solution Chemistry*, **23**: 831-848.
 35. H. L. Friedman, C. V. Krishnan, (1973) Thermodynamics of ionic hydration. In: F. Franks (Ed.), *Aqueous Solutions of Simple Electrolytes*, Boston, MA: Springer US, p1-118.
 36. W. Devine, B. M. Lowe, (1971) Viscosity B-coefficients at 15 and 25°C for glycine, alanine, 4-amino-n-butryic acid, and 6-amino-



- n-hexanoic acid in aqueous solution, *Journal of the Chemical Society A: Inorganic, Physical, Theoretical*, 2113-2116.
37. T. S. Sarma, J. C. Ahluwalia, (1973) Experimental studies on the structures of aqueous solutions of hydrophobic solutes, *Chemical Society Reviews*, **2**: 203-232.
38. I. Pitkänen, J. Suuronen, J. Nurmi, (2010) Partial molar volume, ionization, viscosity and structure of glycine betaine in aqueous solutions, *Journal of Solution Chemistry*, **39**: 1609-1626.
39. M. M. Bhattacharyya, M. Sengupta, (1988) Ion-Solvent interaction of amino acids. The role of the “zwitterionic” and the “ionic” forms in the modification of water structure over the temperature range 25-45°C, *Bulletin of the Chemical Society of Japan*, **61**: 4107-4112.
40. A. Z. Tasic, B. D. Djordjevic, D. K. Grozdanic, N. Radojkovic, (1992) Use of mixing rules in predicting refractive indexes and specific refractivities for some binary liquid mixtures, *Journal of Chemical and Engineering Data*, **37**: 310-313.
41. E. M. Fenton, (1990) The chemistry of macrocyclic ligand complexes Edited by L. F. Lindoy Cambridge University Press, Cambridge, 1989, pp viii +269 £45.00. SUS 0 521 25261 X, *Journal of Coordination Chemistry*, **21**: 87-87.
42. D. Ekka, M. N. Roy, (2012) Conductance, a contrivance to explore ion association and solvation behavior of an ionic liquid (tetrabutylphosphonium tetrafluoroborate) in acetonitrile, tetrahydrofuran, 1,3-dioxolane, and their binaries, *The Journal of Physical Chemistry B*, **116**: 11687-11694.
43. D. Ekka, T. Ray, K. Roy, M. N. Roy, (2016) Exploration of solvation consequence of ionic liquid [Bu₄PCH₃SO₃] in various solvent systems by conductance and FTIR study, *Journal of Chemical and Engineering Data*, **61**: 2187-2196.

SUPPLEMENTARY INFORMATION

Table S1: Density (ρ) of (TH+H₂O+CAFFEINE) and (AA+H₂O+CAFFEINE systems in aqueous caffeine solutions of mass fractions W₁=0.001, W₂=0.003, W₃=0.005, at 288.15K, 298.15 K, 308.15 K, and 318.15 K.

Density (ρ) $\times 10^{-3}$ Kg.m ⁻³			
TH+H ₂ O+CAFFEINE			
288.15K	298.15K	308.15K	318.15K
$w_1=0.001$			
1.00011	0.99820	0.99490	0.99184
1.00112	0.99917	0.99581	0.99289
1.00221	1.00019	0.99680	0.99415
1.00339	1.00130	0.99783	0.99548
1.00467	1.00249	0.99891	0.99685
$w_2=0.003$			
1.00013	0.99826	0.99493	0.99192
1.00116	0.99924	0.99583	0.99296
1.00225	1.00032	0.99681	0.99422
1.00344	1.00147	0.99788	0.99552
1.00474	1.00270	0.99907	0.99697
$w_3=0.005$			
1.00014	0.99826	0.99494	0.99194
1.00120	0.99928	0.99586	0.99302
1.00240	1.00039	0.99689	0.99434
1.00369	1.00160	0.99801	0.99585
1.00524	1.00299	0.99931	0.99727
AA+H ₂ O+CAFFEINE			
$w_1=0.001$			
0.99945	0.99755	0.99436	0.99115
0.99982	0.99780	0.99469	0.99131
1.00024	0.99808	0.99506	0.99152
1.00069	0.99838	0.99548	0.99176
1.00116	0.99869	0.99596	0.99199
$w_2=0.003$			
0.99948	0.99756	0.99439	0.99118
0.99984	0.99787	0.99477	0.99134
1.00027	0.99826	0.99527	0.99154
1.00075	0.99869	0.99586	0.99183
1.00128	0.99911	0.99656	0.99224

Table S2: Refractive Index (n_D) of (TH+H₂O+CAFFEINE) and (AA+H₂O+CAFFEINE systems in aqueous caffeine solutions of mass fractions W₁=0.001, W₂=0.003, W₃=0.005, at 288.15K, 298.15 K, 308.15 K, and 318.15 K.

Molality (Mol/Kg)	288.15K	298.15K	308.15K	318.15K
	Refractive Index (n_D)			
	TH+H ₂ O+CAFFEINE			
$w_1=0.001$				
0.020	1.3322	1.3320	1.3319	1.3315
0.040	1.3331	1.3328	1.3326	1.3322
0.060	1.3339	1.3335	1.3332	1.3329
0.080	1.3346	1.3341	1.3338	1.3335
0.100	1.3357	1.3351	1.3345	1.3342
$w_2=0.003$				
0.020	1.3324	1.3320	1.3319	1.3317
0.040	1.3333	1.3328	1.3327	1.3323
0.060	1.3341	1.3336	1.3333	1.3329
0.080	1.3348	1.3342	1.3339	1.3335
0.100	1.3358	1.3352	1.3347	1.3342
$w_3=0.005$				
0.020	1.3329	1.3328	1.3326	1.3324
0.040	1.3338	1.3335	1.3332	1.3329
0.060	1.3346	1.3342	1.3338	1.3335
0.080	1.3353	1.3348	1.3343	1.3341
0.100	1.3362	1.3356	1.3350	1.3347
AA+H₂O+CAFFEINE				
$w_1=0.001$				
0.020	1.3301	1.3299	1.3296	1.3294
0.040	1.3310	1.3307	1.3305	1.3304
0.060	1.3318	1.3315	1.3314	1.3313
0.080	1.3324	1.3322	1.3321	1.3320
0.100	1.3331	1.3329	1.3328	1.3327
$w_2=0.003$				
0.020	1.3324	1.3321	1.3318	1.3316
0.040	1.3330	1.3327	1.3325	1.3324
0.060	1.3334	1.3332	1.3330	1.3328
0.080	1.3338	1.3336	1.3334	1.3332
0.100	1.3343	1.3341	1.3339	1.3337
$w_3=0.0035$				
0.020	1.3327	1.3326	1.3321	1.3319
0.040	1.3334	1.3331	1.3329	1.3327
0.060	1.3338	1.3338	1.3334	1.3332
0.080	1.3342	1.3342	1.3338	1.3337
0.100	1.3348	1.3350	1.3345	1.3343

Table S3: Viscosity (η) of (TH+H₂O+CAFFEINE) and (AA+H₂O+CAFFEINE in aqueous caffeine solutions of mass fractions W₁=0.001, W₂=0.003, W₃=0.005, at 288.15K, 298.15 K, 308.15 K, and 318.15 K.

Molality (Mol/Kg)	288.15K	298.15K	308.15K	318.15K
	Viscosity (η)			
	TH+H ₂ O+CAFFEINE			
$w_1=0.001$				
0.020	1.036860	0.907585	0.741026	0.630020
0.040	1.061274	0.916974	0.754501	0.658506
0.060	1.079435	0.930681	0.765919	0.685004
0.080	1.099854	0.946623	0.777385	0.717983
0.100	1.116165	0.960538	0.793178	0.755289
$w_2=0.003$				
0.020	1.041126	0.911889	0.745311	0.640767
0.040	1.065564	0.927671	0.763043	0.682050
0.060	1.085855	0.941441	0.77659	0.717074
0.080	1.114798	0.955302	0.788093	0.747885
0.100	1.129019	0.973529	0.806115	0.776715
$w_3=0.005$				
0.020	1.045381	0.914014	0.74958	0.642918
0.040	1.076224	0.934086	0.771589	0.684225
0.060	1.096644	0.952145	0.78518	0.719293
0.080	1.125712	0.968203	0.798862	0.752399
0.100	1.14875	0.982336	0.814846	0.781214
AA+H₂O+CAFFEINE				
$w_1=0.001$				
0.020	1.036176	0.911241	0.766172	0.635995
0.040	1.059896	0.924211	0.7877	0.676654
0.060	1.077314	0.935087	0.80713	0.710872
0.080	1.096895	0.948109	0.824476	0.740812
0.100	1.112266	0.956897	0.844001	0.768591
$w_2=0.003$				
0.020	1.068016	0.913373	0.77045	0.640289
0.040	1.104441	0.928522	0.798394	0.680937
0.060	1.134594	0.941626	0.820053	0.717268
0.080	1.160577	0.956897	0.837543	0.745113
0.100	1.184515	0.976413	0.861511	0.770907
$w_3=0.0035$				
0.020	1.074074	0.915506	0.77472	0.648839
0.040	1.112206	0.930701	0.802693	0.689479
0.060	1.143964	0.948118	0.824408	0.723727
0.080	1.173592	0.96346	0.841986	0.755861
0.100	1.198977	0.981045	0.870217	0.790161

Table S4: Apparent molar volume (ϕ_V) and Molar Refraction (R_M) of (TH+H₂O+CAFFEINE) and (AA+H₂O+CAFFEINE) systems in aqueous caffeine solutions of mass fractions $W_1=0.001$, $W_2=0.003$, $W_3=0.005$, at 288.15K, 298.15 K, 308.15 K and 318.15 K.

288.15K		298.15K		308.15K		318.15K		
TH+H ₂ O+CAFFEINE								
Molality (Mol/Kg)	$\phi V \times 10^6$ (m ³ mol ⁻¹)	RM (m ³ mol ⁻¹)	$\phi V \times 10^6$ (m ³ mol ⁻¹)	RM (m ³ mol ⁻¹)	$\phi V \times 10^6$ (m ³ mol ⁻¹)	RM (m ³ mol ⁻¹)	$\phi V \times 10^6$ (m ³ mol ⁻¹)	RM (m ³ mol ⁻¹)
$w_1=0.001$								
0.020	147.3123	39.8525	151.5932	39.9069	157.1107	40.0283	156.0870	40.1079
0.040	145.5608	39.9102	148.8359	39.9554	153.3386	40.0683	149.5283	40.1423
0.060	143.6426	39.9537	147.0812	39.9908	150.7400	40.0941	143.8104	40.1681
0.080	141.5575	39.9826	145.0759	40.0117	148.9378	40.1181	140.0686	40.1800
0.100	139.3056	40.0507	143.0706	40.0727	147.3535	40.1510	137.4199	40.2012
$w_2=0.003$								
0.020	147.8082	39.8735	151.5841	39.9045	156.6046	40.0271	156.5773	40.1266
0.040	145.3062	39.9303	148.3271	39.9526	153.3355	40.0785	150.0192	40.1504
0.060	143.4714	39.9738	145.7370	39.9965	150.9046	40.1046	144.1337	40.1653
0.080	141.3156	40.0023	143.5647	40.0158	148.5576	40.1270	140.6865	40.1784
0.100	138.9011	40.0587	141.4592	40.0752	145.9423	40.1663	137.1047	40.1964
$w_3=0.005$								
0.020	145.8110	39.9275	151.0843	39.9918	156.1016	40.1034	155.5683	40.2027
0.040	143.5592	39.9831	147.3245	40.0273	152.5811	40.1319	148.5058	40.2138
0.060	140.4733	40.0221	144.5673	40.0590	149.5635	40.1560	142.1158	40.2261
0.080	137.8044	40.0465	141.9355	40.0757	146.9230	40.1654	136.5246	40.2307
0.100	133.6009	40.0820	138.5516	40.10 ⁶ 9	143.5282	40.1893	134.0779	40.2388
AA+H ₂ O+CAFFEINE								
$w_1=0.001$								
0.020	162.2547	35.9602	166.0617	36.0089	166.0933	36.0945	172.6654	36.1915
0.040	160.0028	36.0360	165.0591	36.0792	163.3271	36.1721	171.1518	36.2854
0.060	158.4182	36.0999	164.2235	36.1483	161.7344	36.2481	169.8064	36.3675
0.080	157.2505	36.1429	163.5551	36.2067	160.3094	36.3023	168.7554	36.4285
0.100	156.3498	36.1950	163.0537	36.2647	158.8509	36.3542	168.2256	36.4897
$w_2=0.003$								
0.020	162.2498	36.1866	165.5604	36.2266	165.5870	36.3123	175.6765	36.4099
0.040	160.2482	36.2329	163.3044	36.2747	161.8150	36.3679	172.6497	36.4838
0.060	158.4134	36.2568	161.2155	36.3100	158.5459	36.3993	170.9681	36.5163
0.080	156.8705	36.2789	159.6697	36.3339	155.7798	36.4173	168.9923	36.5454
0.100	155.4444	36.3089	158.8425	36.3680	153.0136	36.4413	166.5960	36.5801
$w_3=0.005$								
0.020	161.7494	36.2159	165.0591	36.2757	164.5812	36.3413	175.1720	36.4395
0.040	158.4968	36.2698	161.8004	36.3121	160.3062	36.4054	171.8930	36.5126
0.060	157.2458	36.2937	159.0431	36.3646	156.4168	36.4343	169.1184	36.5520
0.080	155.4944	36.3143	157.1631	36.3859	152.8879	36.4486	166.8483	36.5889
0.100	154.0432	36.3531	154.9020	36.4426	150.5995	36.4919	164.5782	36.6323

Table S5: $(\eta r^l)/\sqrt{c}$ of (TH+H₂O+CAFFEINE) and (AA+H₂O+CAFFEINE) systems in aqueous caffeine solutions of mass fractions W₁=0.001, W₂=0.003, W₃=0.005, at 288.15K, 298.15 K, 308.15 K, and 318.15 K.

$(\eta r^l)/\sqrt{c}$					
TH+H ₂ O+CAFFEINE					
Molality (Mol/Kg)	288.15K	298.15K	308.15K	318.15K	
w ₁ =0.001					
0.020	0.3250	0.1244	0.1723	0.9950	
0.040	0.3529	0.1406	0.2150	0.9615	
0.060	0.3630	0.1775	0.2400	0.9809	
0.080	0.3872	0.2169	0.2638	1.0606	
0.100	0.3983	0.2434	0.3050	1.1622	
w ₂ =0.003					
0.020	0.3233	0.1407	0.1711	1.0387	
0.040	0.3514	0.1877	0.2428	1.1039	
0.060	0.3701	0.2162	0.2743	1.1573	
0.080	0.4233	0.2420	0.2934	1.1972	
0.100	0.4238	0.2809	0.3408	1.2340	
w ₃ =0.005					
0.020	0.3379	0.1406	0.1698	1.0340	
0.040	0.3935	0.2114	0.2704	1.0994	
0.060	0.4049	0.2548	0.2966	1.1529	
0.080	0.4536	0.2841	0.3229	1.2071	
0.100	0.4788	0.3039	0.3579	1.2421	
AA+H ₂ O+CAFFEINE					
w ₁ =0.001					
0.020	0.3201	0.1533	0.4181	1.0715	
0.040	0.3460	0.1811	0.4444	1.1258	
0.060	0.3542	0.1977	0.4725	1.1721	
0.080	0.3766	0.2228	0.4940	1.2068	
0.100	0.3859	0.2305	0.5272	1.2384	
w ₂ =0.003					
0.020	0.5143	0.1524	0.4154	1.0326	
0.040	0.5466	0.1925	0.4857	1.0939	
0.060	0.5699	0.2170	0.5181	1.1587	
0.080	0.5859	0.2483	0.5337	1.1796	
0.100	0.6000	0.2911	0.5815	1.2011	
w ₃ =0.005					
0.020	0.5413	0.1523	0.4127	1.1086	
0.040	0.5738	0.1925	0.4829	1.1462	
0.060	0.5985	0.2365	0.5154	1.1851	
0.080	0.6233	0.2653	0.5312	1.2289	
0.100	0.6380	0.2994	0.5971	1.2925	

Table S6: Molar conductivities (TH+H₂O+CAFFEINE) and (AA+H₂O+CAFFEINE) systems in aqueous caffeine solutions of mass fractions W₁=0.001, W₂=0.003, W₃=0.005, at 288.15K, 298.15 K, 308.15 K, and 318.15 K.

Molar conductivities (S cm² mol⁻¹)			
TH+H₂O+CAFFEINE			
Molarity (moles/l)	0.001	0.003	0.005
288.15K			
0.02	14.7300	45.8800	51.1500
0.04	8.5725	23.7125	29.0750
0.06	5.9717	16.1183	19.7333
0.08	4.5288	12.3150	15.0125
0.1	3.7520	3.9600	12.4000
298.15K			
0.02	28.005	58.2500	60.0000
0.04	14.7825	30.9000	31.2750
0.06	10.10167	21.1667	21.4167
0.08	7.855	16.2500	16.5375
0.1	6.856	13.2000	13.8400
308.15K			
0.02	28.005	75.38	78.8
0.04	14.7825	37.85	39.85
0.06	10.10167	26.03333	26.83333
0.08	7.855	19.6875	20.5
0.1	6.856	16.1	16.35
318.15K			
0.02	30.51	93.5	96.5
0.04	17.1525	46.5	50.75
0.06	11.68333	31.16667	37.33333
0.08	9.175	24.2	31
0.1	7.86	20.17	26.5
AA+H₂O+CAFFEINE			
Molarity (moles/l)	0.001	0.003	0.005
288.15K			
0.04	1.7085	2.5625	4.03
0.06	0.5187	1.362167	2.206667
0.08	0.2279	0.652875	1.28425
0.1	0.1000	0.258	0.7294
298.15K			
0.02	4.2415	7.725	11.627
0.04	1.8825	3.1975	4.6975
0.06	0.663	1.63433	2.566667
0.08	0.13125	0.851	1.5525
0.1	0.01668	0.3327	0.8314
308.15K			
0.02	4.8675	11.99	14.255
0.04	2.1835	5.2125	5.883
0.06	0.814	2.798333	3.304667
0.08	0.3505	1.55125	1.6
0.1	0.1615	0.4225	0.94
318.15K			
0.02	5.41	14.96	16.2
0.04	2.408	6.62	7.3525
0.06	0.955333	3.51	4.237667
0.08	0.425125	1.81125	2.47875
0.1	0.2952	0.5279	1.01

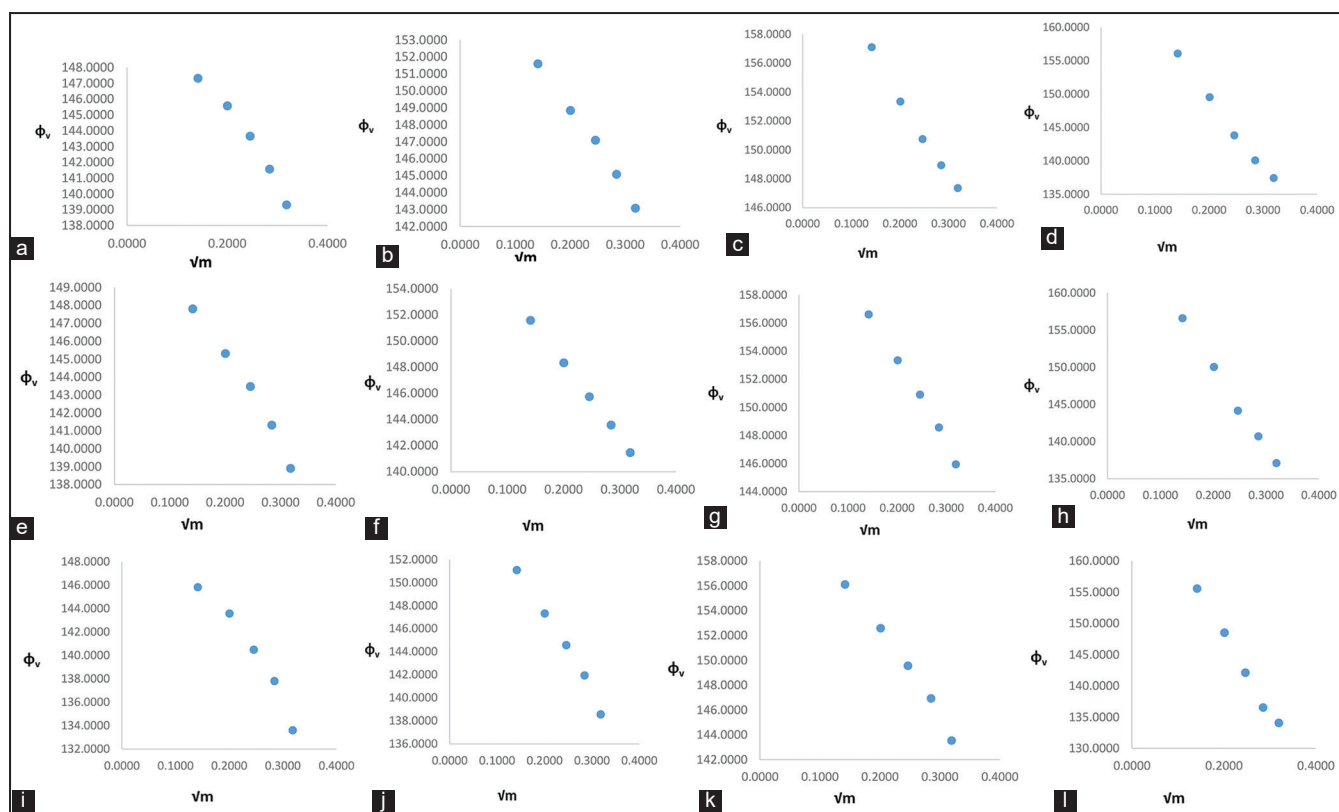


Figure S1: (a-l) Plot of (ϕ_v) versus \sqrt{m} of (TH + H₂O+CAFFEINE) in aqueous caffeine solutions of mass fractions W₁=0.001, W₂=0.003, W₃=0.005, at 288.15K, 298.15 K, 308.15 K and 318.15 K.

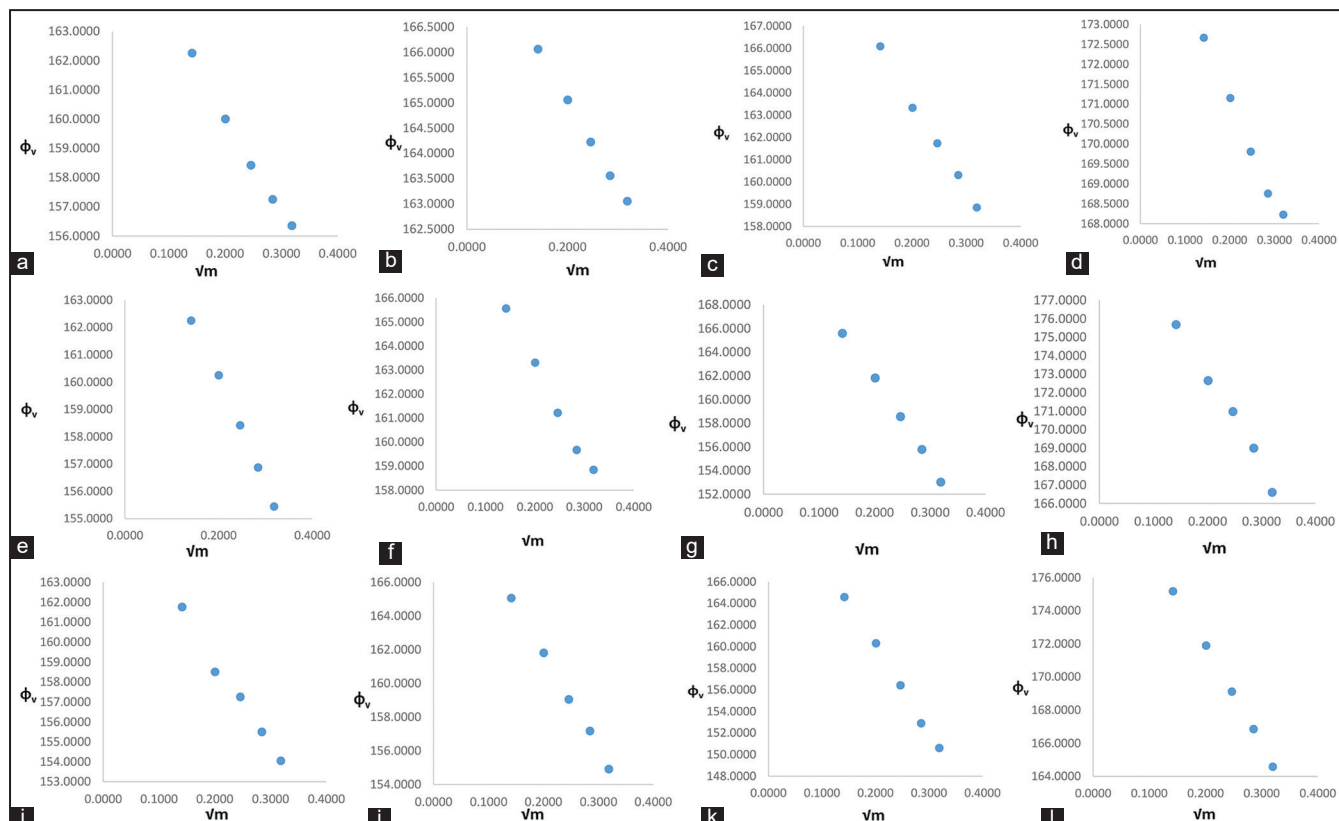


Figure S2: (a-l) Plot of (ϕ_v) versus \sqrt{m} of (AA+H₂O+CAFFEINE) in aqueous caffeine solutions of mass fractions W₁=0.001, W₂=0.003, W₃=0.005, at 288.15K, 298.15 K, 308.15 K, and 318.15 K.

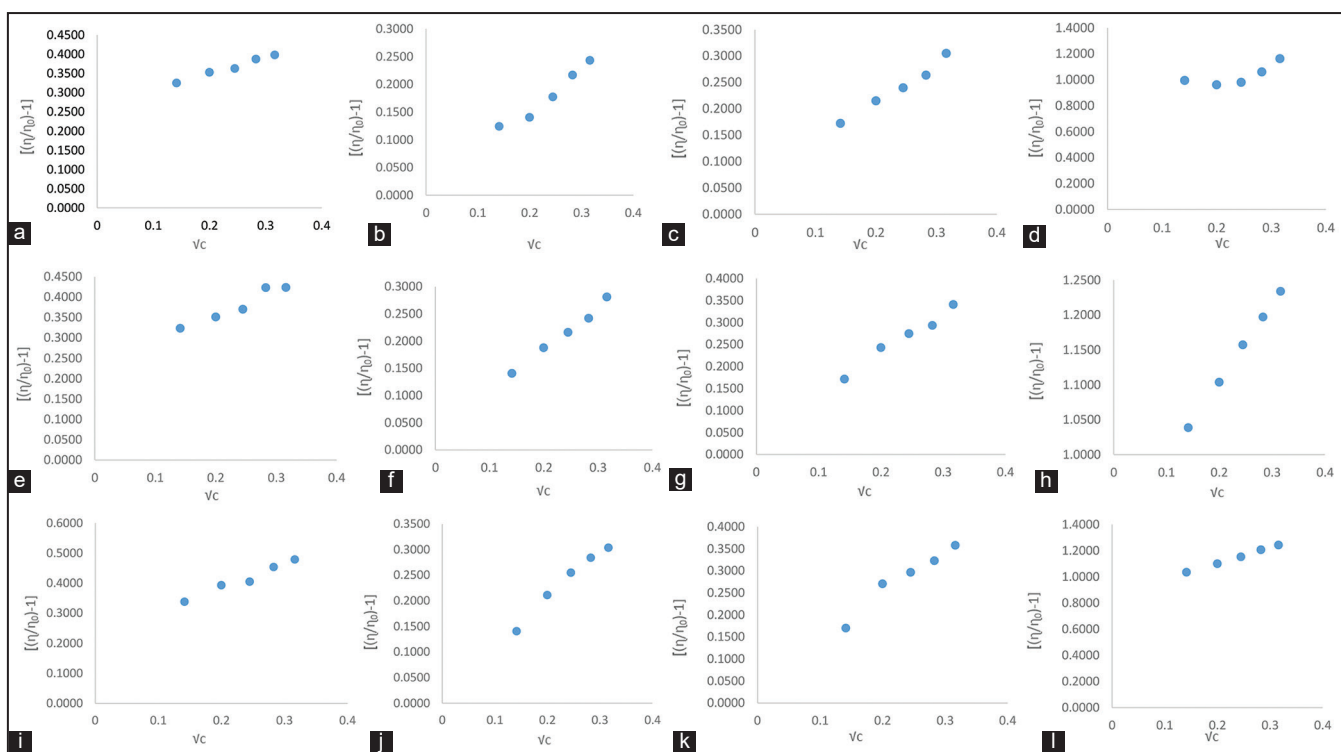


Figure S3: (a-l) Plot of $[(\eta/\eta_0)-1]/\sqrt{c}$ versus \sqrt{c} of (TH + H₂O+CAFFEINE) in aqueous caffeine solutions of mass fractions W₁=0.001, W₂=0.003, W₃=0.005, at 288.15K, 298.15 K, 308.15 K, and 318.15 K.

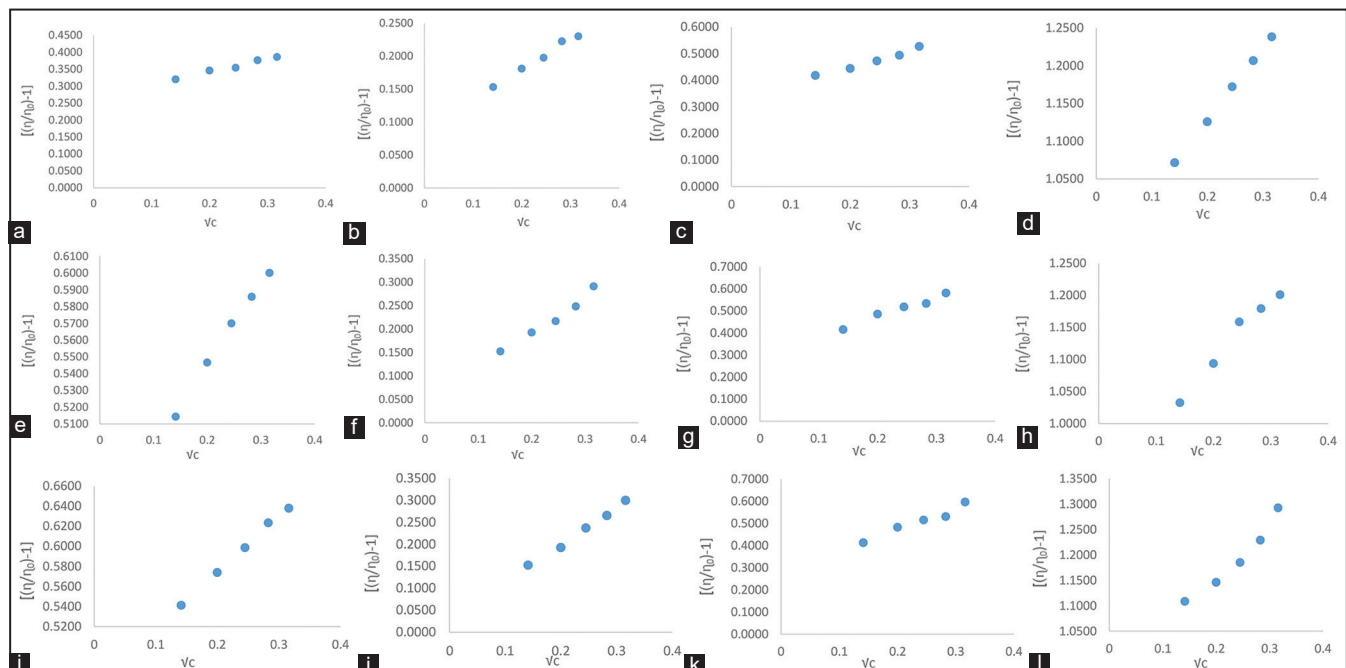


Figure S4: (a-l) Plot of $[(\eta/\eta_0)-1]/\sqrt{c}$ versus \sqrt{c} of (AA + H₂O+CAFFEINE) in aqueous caffeine solutions of mass fractions W₁=0.001, W₂=0.003, W₃=0.005, at 288.15K, 298.15 K, 308.15 K, and 318.15 K.

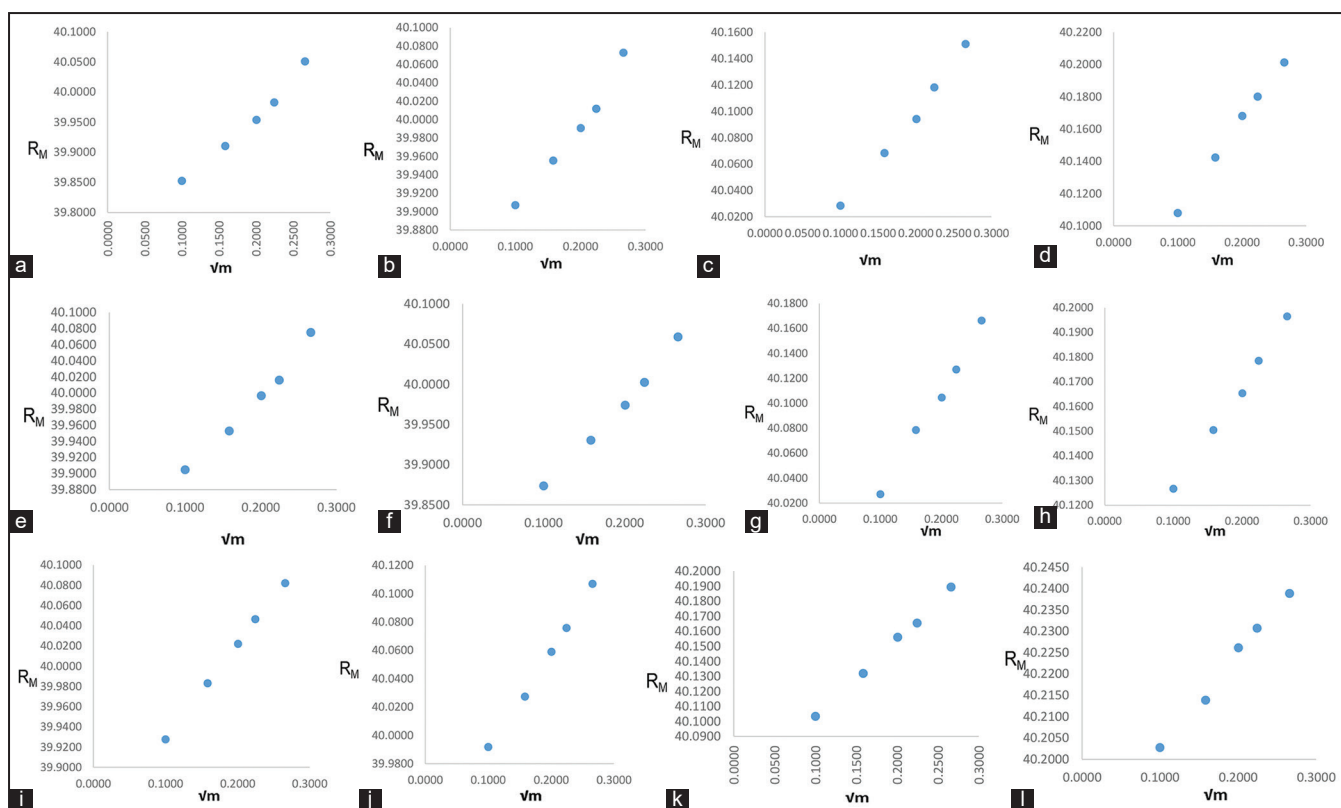


Figure S5: (a-l) Plot of (R_M) Vs \sqrt{C} of ($\text{TH} + \text{H}_2\text{O} + \text{CAFFEINE}$) in aqueous caffeine solutions of mass fractions $W_1=0.001$, $W_2=0.003$, $W_3=0.005$, at 288.15K, 298.15 K, 308.15 K, and 318.15 K.

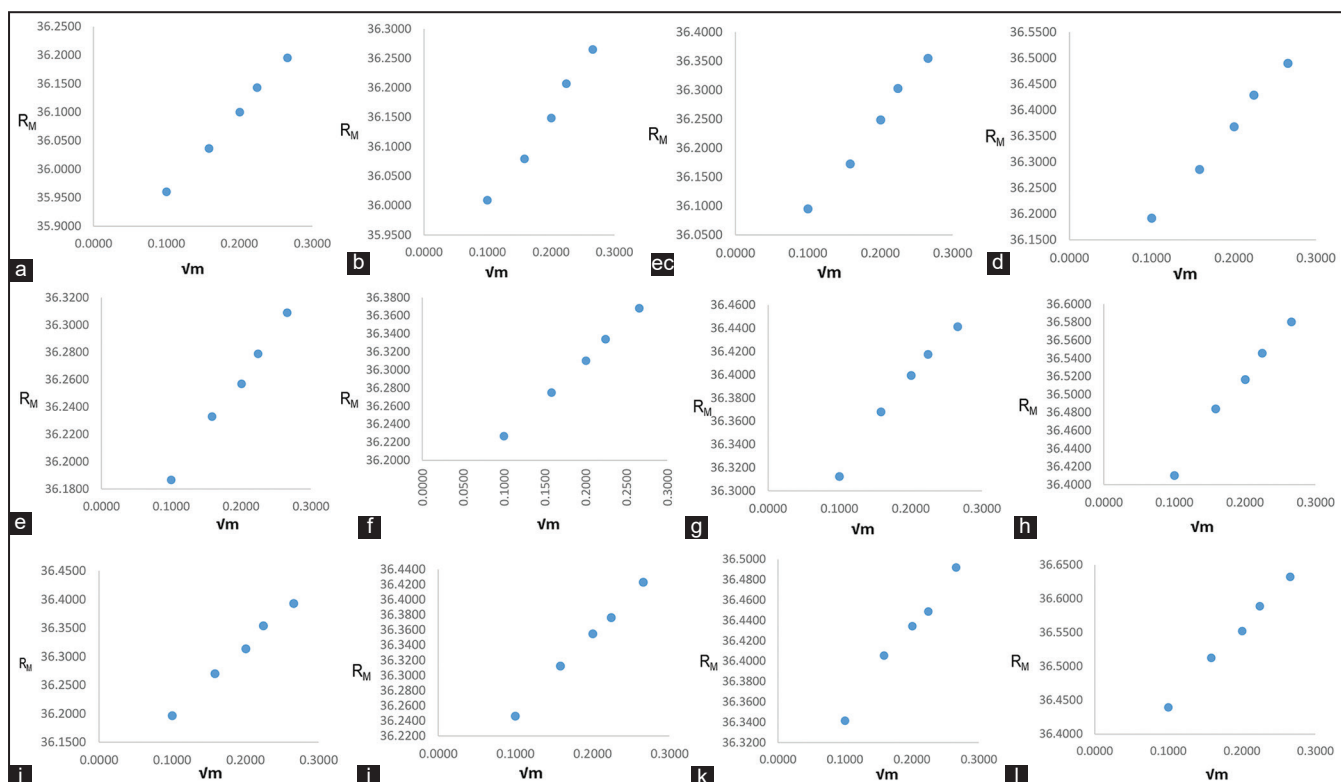


Figure S6: (a-l) Plot of (R_M) versus $\sqrt{\text{cof}}$ ($\text{AA} + \text{H}_2\text{O} + \text{CAFFEINE}$) in aqueous caffeine solutions of mass fractions $W_1=0.001$, $W_2=0.003$, $W_3=0.005$, at 288.15K, 298.15 K, 308.15 K, and 318.15 K.